The Effect of Cloud-Radiation Interaction on the East Asia Climate as Simulated From the SUNYA Regional Climate Model

Wei Gong* and Wei-Chyung Wang
Atmospheric Sciences Research Center, State University of New York at Albany
251 Fuller Rd., Albany, NY 12203 U.S.A.
Telephone: (518) 437-8716; Fax: (518) 437-8713
Email: gong@climate.cestm.albany.edu

1. Introduction

Regional climate model (RCM) has been used in many regions around the world to study climate characteristics and to simulate severe climate events (e.g. Walsh and Waterson, 1997; Jenkins, 1997; Giorgi and Mearns, 1999a.; Wang et al., 2000). However, most studies have focused on the model's performance in reproducing circulation fields and surface climatology, such as air temperature and precipitation. There is generally a lack of model validation on clouds and the associated physical and dynamical fields.

Simulation of clouds is perhaps the largest cause for uncertainty in simulating climate (Cess et al., 1990). Cloud cover and its radiative properties are critical not only in affecting the surface energy budget that determines the surface temperature, but also the vertical temperature profiles through vertical heating/cooling. Examination of model performance in simulating clouds and their radiative properties was occasionally performed for RCMs. For example, in an intercomparison study of three RCMs, Leung et al. (1999) found that differences among the models are mainly due to cloud-radiation interaction with respect to cloud cover and its radiative properties. Specifically, they found that the National Center for Atmospheric Research (NCAR) Regional Climate Model version 2 (RegCM2) was due to the excessive ice cloud cover at the upper troposphere. As a result, Giorgi et al. (1999b) adjusted the cloud cover scheme in order to better simulate climate over East Asia.

There have been several versions of the State University of New York at Albany (SUNYA) RCM. Wang et al. (2000) validated the performance of the RCM0 in the East Asia monsoon, and showed the model is capable of reproducing the seasonal variation of circulation and the Meiyu rainbelt. Gong and Wang (2000) examined the model biases in the large-scale circulation, and found that the excessive inversion cloud is responsible for the model's cold bias over some regions. Gong et al. (2000) has recently incorporated a land surface process model into RCM0 together with CCM3 radiation scheme (here referred to as RCM1), and find that the simulated diurnal cycle of surface air temperature and daily variation of Meiyu precipitation are much more realistic, due mainly to improved land surface-atmosphere interaction.

Nevertheless, the radiation package in the RCM1 still uses the prescribed profile of cloud liquid/ice water content (CWC), which is based on the algorithms in CCM3 with slight modification. This profile represents, to some extent, the climatological mean value (referred as *climatological* CWC). On the other hand, the RCM will be ultimately used for climate predictions, e.g., climate change due to greenhouse gases and anthropogenic sulfate aerosols. For a changed climate, CWC might be significantly different from the present climate. It is thus necessary to correct the inconsistency.

In this study, we couple the prognostic CWC generated in the RCM's explicit moisture scheme with the radiation scheme interactively (referred to as *prognostic* CWC). This model version, designated as RCM1.5, is used to simulate both the 1998 and 1991 East Asia summer monsoon, when severe flooding events occurred in the Yangtze River and Yangtze-Huai River valley (YHRV). Both climatological and prognostic CWCs are used in the simulation. The model surface climatology and cloud are verified against the surface observation and International Satellite Cloud Climatology Project (ISCCP)-D1 satellite data. Section 2 briefly describes the model physics, focusing on the interaction between CWC and radiation. In section 3, we show the effect of cloud-radiation interaction on the simulation of East Asia summer monsoon. Finally, in section 4 we present our conclusions.

2. Model Physics

The SUNYA RCM uses a radiation package adopted from NCAR CCM3 (Kiehl et al., 1996). For the precipitation physics it adopts the Grell cumulus scheme and mix-phase explicit moisture scheme that separately calculates the cloud liquid water and cloud ice contents (Grell et al., 1993). The land surface and turbulence processes are parameterized using the Simplified Simple Biosphere model (SSiB) and the Mellor-Yamada PBL scheme, respectively (see Xue et al., 1996).

* Corresponding author

As mentioned in the introduction, the RCM1.5 uses the prognostic CWC in the radiation package. In the CCM3 radiation package, CWC influences the solar radiation through optical depth (τ)

$$\tau_l = CWP\left[a_l^\lambda + \frac{b_l^\lambda}{r_{el}}\right](1 - f_{ice})$$

for cloud liquid water (1a)

and

$$\tau_i = CWP\left[a_i^\lambda + \frac{b_i^\lambda}{r_{ei}}\right]f_{ice}$$

for cloud ice water (1b)

Here, CWP is cloud water path gm^{-2} and a and b are constants. Subscripts l and i denote the cloud liquid and ice water,

interval. f_{ice} is the fraction of cloud ice water content. CWC also modifies the longwave radiation through the cloud emissivity (ε_{cld})

$$\varepsilon_{cld} = 1 - e^{-D\kappa_{abs}CWP} \qquad (2)$$

Where D is a diffusive factor (1.66), κ_{abs} is the cloud longwave absorption coefficient (m^{2}g^{-1}).

The cloud cover is basically diagnosed from relative humidity and vertical velocity according to various cloud types (Liang and Wang, 1995; Gong and Wang, 2000). In practice, for the prognostic CWC it will be set to zero in the RCM, when total CWP (the sum of liquid and ice) is less than 0.01 gm^{-2} in a model layer.

3. Effect of cloud water content

For simulation of the East Asia summer monsoon, the model configuration, such as domain, horizontal resolution and vertical levels, are the same as those described in Gong et al. (2000). Twice daily, the driving fields for atmospheric variables are derived from the European Center for Medium-Range Weather Forecast (ECMWF)-Tropical Ocean Global Atmosphere (TOGA) objective analysis while the sea surface temperature is generated from the National Center for Environmental Prediction (NCEP)-NCAR analysis. Two experiments are conducted: CC and PC, which denote the simulations with climatological and prognostic CWC, respectively. As in Wang et al. (2000), statistics are calculated for three regions and the domain average (average of three regions). For the daily variation, only the result for YHRV will be presented.

Figure 1 shows the daily precipitation over YHRV for the period from May 1 to August 31, 1998. It can be seen that the model captures reasonably well the daily variation for this flooding event for both CC and PC. The monthly precipitation spatial pattern is also reasonably well simulated by CC and PC for each month of 1998 (not shown). However, the maximum and minimum surface air temperatures were under-predicted by PC (Fig. 2), while they are simulated reasonably well by CC.

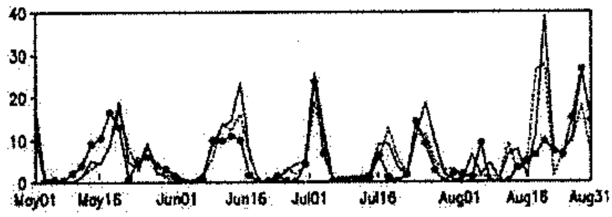

Fig. 1: The daily variation of precipitation (mm) over YHRV during the period from May 1 to August 31, 1998. Solid with dark circle is for observation from WMO stations; solid for CC; and dashed for PC.

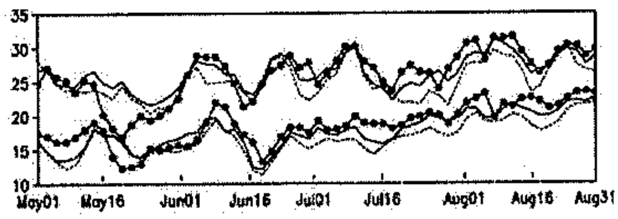

Fig. 2: Same as in Fig. 1, except for the maximum and minimum surface air temperature (°C).

To explore the reason why PC produced a colder surface air temperature, we compare the simulated total cloud cover, cloud water content and optical depth between the two cases, and also compare them with observations. For the latter, we use the ISCCP-D1 satellite data. Because this dataset is only available for years prior to 1997, cases CC and PC for 1991 were rerun for May and June of that year. Again, for 1991 colder surface maximum and minimum air temperatures were found in PC (not shown).

In the comparison of the simulation against the satellite data, the simulated cloud cover, CWC and optical depth, need be processed the same way as those from the satellites. The methodology for total cloud, its CWC and optical depth is adopted from Yu et al. (1996). This method calculates these quantities according to the random overlap assumption between each cloud layer. In addition, the method suggested by Klein and Jakob

(1999) is used to adjust the cloud-top pressure for those high clouds with emissivity less than unity. This method was derived following the procedure that ISCCP used to calculate the cloud top pressure.

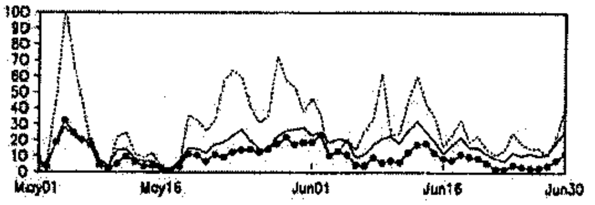

Fig. 3: The daily variation of cloud optical depth (unity) over YHRV during the period from May 1 to June 30, 1991. Solid with dark circle is for ISCCP-D1 satellite data; solid for CC; and dashed for PC.

As can be seen in Fig. 3, there is a large difference in the optical depth between CC and PC. For the case CC, the cloud optical depth generally follows the observation although it is still over-predicted in June 1991. Case PC, however, over-predicts the optical depth by about 3-4 times of the observed value over YHRV. With larger optical depth, the cloud will reflect more solar flux during the daytime, and thus lead to a colder maximum surface air temperature.

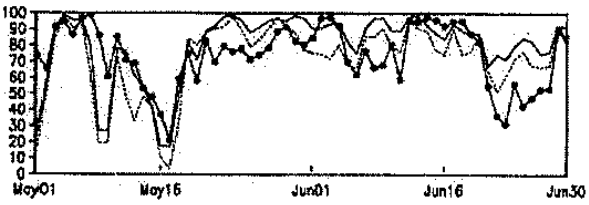

Fig. 4: Same as in Fig. 3, except for the cloud cover (percent).

Generally, the daily variation of cloud cover for both CC and PC are well simulated for the two months of 1991 (Fig. 4). However, both cases under-predict cloud cover in North China. This can be partially explained by the fact that the region includes part of the buffer zone. Previous studies (e.g. Giorgi et al., 1993; and Gong et al., 2000) have indicated that RCMs generally under-predict cloud cover in the lateral buffer zone. In addition, case PC simulates less cloud cover than CC. The main reason is that case PC simulates a drier atmosphere because of the reduced turbulence related to colder surface temperature during daytime. Hence, the smaller cloud amount explains the colder minimum temperature for case PC during the night since more longwave flux from the surface can emit into the atmosphere.

Figure 5 shows the vertical profile of CWP, which was used in the radiation package, over YHRV for June 1991. It can be seen that case PC produces a much larger CWP, consistent with Fig. 3, in the middle troposphere with maximum around 725 hPa. Note that the corresponding CWC profile, calculated in the presence of cloud, is almost uniformly distributed between levels from 525 hPa to 970 hPa. Therefore, the peak of CWP at middle troposphere is mainly due to the larger distance between model levels. The explanation for the excessive CWC is still not clear because it involves feedback among many dynamical and physical processes in the model. In addition, the observed vertical profile of CWC is not available. We will examine this in the future.

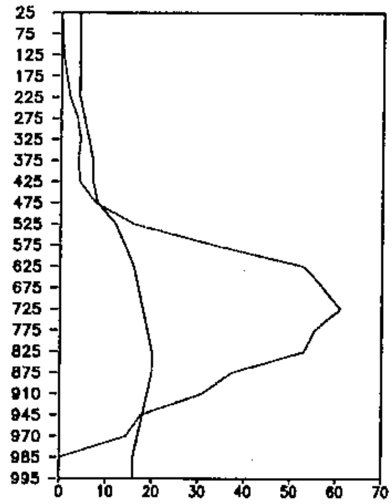

Fig. 5: The vertical profile of cloud water path (gm^{-2}). Solid is for CC; and dashed for PC.

4. Conclusion

In this study, we used the SUNYA regional climate model to investigate the effect of cloud-radiation on the simulation of the East Asia summer monsoon. The study relaxed a condition of using climatological cloud water in radiation calculation. Two experiments with climatological and prognostic cloud water contents are conducted for both 1998 and 1991 when severe flooding events occurred in East Asia. In general, both experiments reproduce well the precipitation and cloud cover in their spatial pattern and daily variation. The experiment with climatological cloud water content reproduces reasonably well the maximum and minimum surface air temperature and the total cloud optical depth.

However, the model with prognostic cloud water predicts excessive cloud water compared with ISCCP-D1 satellite data. As a result, the maximum surface air temperature is colder, which also leads to a drier atmosphere, resulting in less cloud cover. The latter also leads to a cooler surface air temperature during the night. The reason why excessive cloud water content is simulated remains to be further explored.

REFERENCES

Cess, R. D, et al., 1990: Intercomparison and interpretation of climate feedback processes in 19 atmospheric general circulation models. *J. Geophys. Res.*, **95**, 16, 601-16,615.

Giorgi, F., and L. O. Mearns, 1999a: Introduction to special section: Regional climate model revisited. *J. Geophys. Res.*, **104**, 6335-6352.

Giorgi, F., M. R. Marinucci, and G. T. Bates, 1993: Development of a second-generation Regional Climate Model (RegCM2). Part II: Convective processes and assimilation of lateral boundary conditions. *Mon. Wea. Rev.*, **121**, 2814-2832.

Giorgi, F., Y. Huang, K. Nishizawa, and C. Fu, 1999b: A seasonal cycle simulation over eastern Asia and its sensitivity to radiative transfer and surface processes. *J. Geophys. Res.*, **104**, 6403-6423.

Gong, W., and W.-C. Wang, 2000: A regional model simulation of the 1991 severe precipitation event over the Yangtze-Huai River Valley. Part II: Model bias. *J. Climate*, **13**, 93-108.

Gong, W., W.-C. Wang, and Y. Xue, 2000: The effect of land surface-atmosphere interaction on the East Asia summer monsoon as simulated from the SUNYA regional climate model. Submitted to *Climate Dynamics*.

Grell, J., F. Dudhia, and D. Stauffer, 1993: A description of the fifth generation Penn State/NCAR Mesoscale Model (MM5). NCAR Tech. Note NCAR/TN-398+IA, 122pp.

Jenkins, G. S., 1997: The 1988 and 1990 summer season simulations for West Africa using a regional climate model. *J. Climate*, **10**, 1255-1272.

Kiehl, J. T., J. J. Hack, G. B. Bonan, B. A. Boville, B. P. Briegleb, D. L. Williamson, and P. J. Rasch, 1996: Description of the NCAR Community Climate Model (CCM3). NCAR Tech. Note, NCAR/TN-420+STR, 152pp.

Klein, S., and C. Jakob, 1999: Validation and sensitivities of frontal clouds simulated by the ECMWF model. *Mon. Wea. Rev.*, **127**, 2514-2531.

Leung, L. R., S. J. Ghan, Z.-C. Zhao, Y. Luo, W.-C. Wang, and H.-L. Wei, 1999: Intercomparison of regional climate models for simulation of the 1991 summer monsoon in East Asia. *J. Geophys. Res.*, **104**, 6425-6454.

Liang, X.-Z., and W.-C. Wang, 1995: A GCM study of the climatic effect of 1979-1992 ozone trend. *Atmospheric Ozone as a Climate Gas*, NATO ASI Series. W.-C. Wang and I. S. A. Isaksen, Eds., Springer-Verlag, 259-288.

Walsh, K., and I. G. Waterson, 1997: Tropical cyclone-like vortices in a Limited Area Model: Comparison with observed climatology. *J. Climate*, **10**, 2240-2259.

Wang, W.-C., W. Gong, and H.-L. Wei, 2000: A regional model simulation of the 1991 severe precipitation event over the Yangtze-Huai River Valley. Part I: Precipitation and circulation statistics. *J. Climate*, **13**, 74-92.

Xue, Y., M. J. Fennessy, and P. J. Sellers, 1996: Impact of vegetation properties on U.S. summer weather prediction. *J. Geophy. Res.*, **101**, 7419-7430.

Yu, W., M. Doutriaux, G. Sèze, H. Le Treut, and M. Desbois, 1996: A methodology study of the validation of clouds in GCMs using ISCCP satellite observations. *Clim. Dynamics*, **12**, 389-401.